Applied Catalysis B: Environmental 165 (2015) 328–334

Contents lists available at ScienceDirect

Applied Catalysis B: Environmental

journal homepage: www.elsevier.com/locate/apcatb

The effect of NOM to TiO_2: interactions and photocatalytic behavior

Marios Drosos*, Meijie Ren, Fritz H. Frimmel

Chair of Water Chemistry and Water Technology, Karlsruhe Institute of Technology, Engler-Bunte-Ring 1, Building 40.11, 76131 Karlsruhe, Germany

ARTICLE INFO

Article history:
Received 12 July 2014
Received in revised form 1 October 2014
Accepted 7 October 2014
Available online 28 October 2014

Keywords:
NOM
TiO_2
Photocatalysis
EPR
SEC-OCD.

ABSTRACT

Natural organic matter (NOM) is ubiquitous in aquatic environment, which plays a predominant role in the sorption of pharmaceuticals onto the TiO_2 nanoparticles. It is a matter of concern whether NOM could act as a surface sensitizer of TiO_2 or not. In this context, the role of NOM is investigated for the photocatalytic degradation of carbamazepine (CBZ) using TiO_2. Four different ratios of NOM:TiO_2 were used varying from 400 $\mu g\,g^{-1}$ to 400 $mg\,g^{-1}$. The findings reveal that small amounts of NOM could enhance the TiO_2 efficiency up to 8%. Electron paramagnetic spectroscopy (EPR), along with size exclusion chromatography with dissolved organic carbon detection (SEC-OCD) and nuclear magnetic resonance spectroscopy (NMR) reveal the occurring mechanism. TiO_2 binds small molecular size fractions of NOM and breaks aromatic bonds of adsorbed NOM transforming it to stranded alkyl groups. This modified TiO_2 bears a significant amount of electrons (e^-) and lesser holes (h^+) than the purified TiO_2 and when irradiated, produces hydroxyl radicals which degrade CBZ.

1. Introduction

Titanium oxide is used in a wide variety of technological applications where surface properties play a role. It is used in heterogeneous catalysis, as photocatalyst; in solar cells for the production of hydrogen and electric energy, as white pigment, as corrosion-protective or optical coating, as spacer material in magnetic spin-value systems, and it is important in earth sciences [1].

By far, the most actively pursued applied research on TiO_2 is its use for photo-assisted degradation of organic molecules. TiO_2 is a semiconductor where the electron–hole pair, created upon irradiation with sunlight, became separated and the resulting charge carriers migrate to the surface. These react with adsorbed water and oxygen to produce radical species, which attack any adsorbed organic molecule and can, ultimately, lead to their complete decomposition into CO_2 and H_2O [2].

Photocatalysis based on TiO_2 has been intensively investigated in order to improve photocatalytic efficiency for different applications such as decomposition of various organic pollutants in aqueous media [3]. Studies on the doping of non-metal and transition-metal ions into TiO_2 have become attractive in the area of photocatalysis [4].

Natural organic matter (NOM) is ubiquitous in aquatic environment and plays a predominant role in the sorption of toxic substances onto the TiO_2 nanoparticles (NPs) [5]. Once released in the environment, NPs will inevitably interact with abundant NOM [6]. Fulvic acid (FA) and humic acid (HA) are the main constituents of NOM from water resources responsible for water color and odor [7], and also responsible for membrane fouling in water treatment [8]. It is reported that TiO_2 has a strong affinity for HA [9–11], especially at a low pH value. Previous investigations showed that certain groups of organic compounds, such as carboxylic acids, strongly adsorb onto the TiO_2 surface at low pH values whilst others, such as alcohols and saturated long-chain aliphatic compounds, do not [12].

The research on the NOM/TiO_2 interactions was so far limited to the photodegradation of NOM by TiO_2 [7,9–11,13–16]. However, it is reported that the removal of Cr(IV), by using TiO_2 photocatalysis, was greatly enhanced when the system contained both HA and Cr(VI) [16] and also that HA coating enhanced the adsorption of Cd(II) to nano-TiO_2 [6].

It is a matter of concern whether NOM could act as a TiO_2 surface sensitizer or not. So far, only activated carbon has been used as a catalyst support for the photocatalytic degradation [17]. Carbon doping has been shown to be more active than doping with nitrogen [18]. For example, Khan et al. [19] first demonstrated the high photoactivity of carbon-doped TiO_2 in the photoelectrochemical context by measuring the rate of water splitting to H_2 and O_2. Previously, it was reported by Doll et al. that low concentrations of NOM could accelerate the degradation of carbamazepine

* Corresponding author.
E-mail addresses: drosos.marios@gmail.com (M. Drosos), meijie.ren@kit.edu (M. Ren), fritz.frimmel@kit.edu (F.H. Frimmel).

http://dx.doi.org/10.1016/j.apcatb.2014.10.017
0926-3373/

due to the photochemical formation of reactive species by NOM, but at higher concentrations of NOM, the acceleration of the degradation decreased [20]. It is suggested that for the best evaluation of the photocatalytic degradation of NOM by TiO_2, NOM should be characterized in detail [13]. Therefore, the aim of this work was to evaluate the photodegradation efficiency of NOM-modified TiO_2 to CBZ, by using a well-characterized lignite humic acid, as a model NOM, to elucidate the effect of NOM to the photocatalytic behavior of TiO_2.

2. Experimental

2.1. Reagents

Millipore Milli-Q Water (resistivity = 18 MΩ cm) and P25 titanium oxide (nano-TiO_2) (Evonik Degussa GmbH, Düsseldorf, Germany) with purity >99.5% were used for all the experiments. The pH adjustments were carried out using NaOH and HNO_3 from Fluka. The fairly homogeneous humic acid, used as NOM model, is a lignite humic acid (LHA2) previously characterized by Drosos et al. [21] and also named $L_{Parental}$HA in [22]. Carbamazepine (99%) was obtained from Sigma Aldrich.

2.2. Purification

In order to obtain a completely DOC-free TiO_2, a purification step was required by baking P25 TiO_2 at 500 °C for 60 min. An aqueous solution (Milli-Q water) of the baked TiO_2 (20 g L^{-1}) was irradiated for 60 min, under a Solar UV Simulator (Oriel Corp., Stratfort, CT, USA) with additional WG 295 filters (6 mm, Schott Glaswerke, Germany). The scheme and detailed description of the solar simulator used for the irradiation experiments was given by Doll et al. [20]. The radiation source was a 1000-W Xe short-arc lamp, which was turned on at least 30 min prior to irradiation in order to insure a constant photon flux.

The irradiated TiO_2 solution was centrifuged at 4000 rpm for 15 min. The filtered TiO_2 was placed into an oven at 60 °C for 24 h, in order to remove moisture completely. The purified TiO_2 was then grained to obtain fine powder. The supernatant was collected and measured by total organic carbon detection (TOC) and size exclusion chromatography with organic carbon detector (SEC-OCD) after filtration using 0.45 μm filter supor 450.

2.3. Samples preparation

One gram of purified TiO_2 was placed in 50 ml of an LHA2 solution at pH 5, stirred overnight and centrifuged at 4000 rpm for 15 min. The supernatant was collected, filtered using 0.45 μm filter supor 450 and measured by total organic carbon detection (TOC) and size exclusion chromatography with organic carbon detector (SEC-OCD). The different LHA2 solutions used were 8000, 800, 80, and 8 mg L^{-1} respectively, giving four TiO_2-LHA2 ratios. By using 50 ml of Milli-Q instead of the LHA2 solution, the TiO_2 obtained was used as a blank (Blank TiO_2). The materials were placed into an oven at 60 °C for 24 h, in order to remove moisture completely and were grained to obtain a fine powder. The four LHA2-modified TiO_2 samples are named here as it follows: (1) LT04 for the LHA2:TiO_2 ratio of 400 μg g^{-1}, (2) LT4 for the 4 mg g^{-1} ratio, (3) LT40 for the 40 mg g^{-1} ratio and (4) LT400 for the 400 mg g^{-1} ratio.

All CBZ samples were prepared by dissolving CBZ in Milli-Q water, stirred for 6 h and placed in an ultrasonic bath for 15 min to ensure complete dissolution.

The catalysis samples were prepared by adding 1 g L^{-1} LHA2-modified TiO_2 material in 10 mg L^{-1} pharmaceutical solution at pH 7. The sample volume was 50 ml. Samples were irradiated by the Solar UV Simulator introduced by Doll et al. [20].

All samples were stirred and irradiated simultaneously from above by a homogenous light field. During photoreaction, samples were collected at different time intervals for analysis. Before irradiation, adsorption was allowed to take place for 30 min in the dark.

2.4. EPR spectroscopy

Electron paramagnetic resonance (EPR) spectra were recorded at liquid-nitrogen temperature (77 K) with a Bruker ER200D spectrometer equipped with an Agilent 5310A frequency counter. Typically, adequate signal-to-noise ratio was obtained after 20–40 scans. Samples were cooled to 77 K and illuminated in the cavity while spectra were recorded. A 450 W lamp (Oriel model 66929) was used as illumination source. EPR samples were prepared by pasting the wet pellet of each material into 5 mm suprasil (Willmad Co.) quartz tube with no further treatment. *g*-values were calibrated versus DPPH, $g = 2.0036$, as described earlier [23].

2.5. SEC-OCD chromatography and TOC analysis

Size exclusion chromatography coupled with organic carbon and UV (254 nm) detector used a TSK HW 50S Column. The mobile phase was 1.5 g L^{-1} $Na_2HPO_4{\cdot}2H_2O$ and 2.5 g L^{-1} KH_2PO_4 with 1 mL min^{-1} flow rate, followed by acidification using 5 mL L^{-1} phosphoric acid 85% with a flow rate of 0.5 mL min^{-1} under nitrogen 5.0 (28 L h^{-1}) with 0.5–1 bar pressure. The contact time in the reactor was 80 s, 60 s UV radiation and rotation time of the reactor 400 rpm. For the determination of the apparent molecular size, calibration using PEGs was performed. In detail, Vo was determined by blue dextran (2×10^6 Da), Vp by methanol and the calibration PEG standards used varied in molecular weight (200 kDa, 100 kDa, 40 kDa, 20 kDa, 10 kDa, 6 kDa, 4 kDa, 1550 Da, 1000 Da, 400 Da, 200 Da). DOC concentrations were measured both by SEC-OCD and a TOC 5000 Carbon Analyzer (Shimadzu).

2.6. NMR spectroscopy

Solid state ^{13}C NMR spectra of powder samples were recorded on a Bruker NMR spectrometer at a resonance frequency of 400 MHz, using a Ramped-Cross Polarization MAS with a spinning speed of 6.8 kHz [24]. A contact time of (1 ms) and a pulse delay of (400 ms) were used. A ramped ^1H-pulse decreasing the power from 100 to 50% was used to circumvent spin modulation of Hartmann–Hahn conditions [24]. At least 50,000 single scans were collected for each sample.

2.7. HPLC analysis

The concentration of CBZ was measured by high-performance liquid chromatography (HPLC) using an HP 1100 HPLC system (column RP 18e, 5 μm; mobile-phase acetonitrile: water 60:40; 1 mL min^{-1}) with detection at 280 nm by a UV detector.

3. Results and discussion

3.1. TOC and samples

LHA2 was proved to contain 44% of carbon both by elemental analysis in [22] and TOC analysis. More information about LHA2 is summarized in Table 1. The adsorbed carbon on 1 g of purified TiO_2 was 160 μg L^{-1} for LT04 and 670 μg L^{-1} for LT4, close to the concentration found in drinking water. The adsorbed carbon for LT40 was 8 mg L^{-1}, and for LT400 was 44 mg L^{-1}, which are values,

Table 1
Summary of LHA2 parameters.

Sample[a]	Elemental composition (%)					Functional groups (mol kg^{-1})		SEC-OCD SUVA
	C	H	N	O	Ash	–COOH	–OH	
Non-purified LHA2	44	4.1	1.6	37.7	12.6	3.6	2.6	3.7
Purified LHA2	41	3.4	2.0	51.4	2.2			

[a]The elemental composition for non-purified LHA2 is obtained from ref. [22] and for purified LHA2 from ref. [21]. Functional groups obtained from ref. [21] and SUVA obtained from Fig. 5A. In this context, the LHA2 used was purified, however both TOC and SEC-OCD reported 44% C and is the value we used to calculate DOC.

found in water rich in DOC and in soil solutions and wastewater, respectively.

3.2. Carbamazepine photocatalysis

We used CBZ in order to obtain information on the photocatalytic behavior of TiO_2 when applied on a system containing NOM. The results in Fig. 1 clearly show that after 2 h irradiation, CBZ was degraded only by 7%, while when TiO_2 was added, degradation reached 85%. When TiO_2 containing LHA2 is used, major differences were observed. For LT400, the degradation reached only 23%, while it reached 55 and 76% for LT40 and LT4, respectively. This indicates that the organic material obviously prohibits the catalytic behavior of TiO_2. However, for LT04, the degradation reached 93%. That is a degradation rate even larger than that observed on purified TiO_2. Fig. 2 shows that for blank TiO_2 the adsorption of CBZ to TiO_2 was only 7% after 2 h, while in the presence of LHA2 there was a higher percentage of adsorption of CBZ to TiO_2 after 2 h of 8% for LT04 and LT4, 10% for LT40 and 15% for LT400. This reveals that in the presence of NOM, the sorbed NOM to TiO_2 can attract CBZ by adsorption, possibly by π–π stacking.

The photocatalytic degradation of CBZ by means of UV light with purified TiO_2 and NOM-modified TiO_2 can be formally described by the Langmuir–Hinshelwood (L–H) kinetic model:

$$r = -\frac{dc}{dt} = -\frac{kKc}{1+Kc} \quad (1)$$

where dc/dt is the degradation rate, k is the apparent reaction rate constant, K is the equilibrium constant of the substance adsorption on the catalyst, and c is the reactant concentration. In case the degraded concentrations of substances exceed the saturation coverage of the catalyst surface, Eq. (1) (i.e. $Kc \gg 1$) simplifies to a zero-order rate equation.

$$r = -\frac{dc}{dt} = k \quad (2)$$

For very low concentrations (i.e. $Kc \ll 1$), the L–H equation simplifies to a pseudo-first-order kinetic law Eq. (3) where k is the pseudo-first-order rate constant.

$$r = -\frac{dc}{dt} = kc \quad \text{or} \quad c_t = c_0\ e^{-kt} \quad (3)$$

In this work, the photocatalytic degradation rate of CBZ was fitted using the pseudo-first-order kinetic law. The rate constants obtained from data shown in Fig. 1 were 0.0005 min^{-1} for CBZ without TiO_2, 0.0013 min^{-1} for LT400, 0.0054 min^{-1} for LT40, 0.0105 min^{-1} for LT4 and 0.0150 min^{-1} for the undoped purified TiO_2 (Blank TiO_2), while it was 0.0175 min^{-1} for LT04. This supports that low concentrations of NOM accelerate the degradation due to the photochemical formation of reactive species, while at higher concentrations of NOM, the acceleration of the degradation decreases, as reported by Doll et al. [20].

3.3. EPR spectroscopy

EPR spectroscopy reveals the differences between the purified TiO_2 and the NOM-modified TiO_2. Under irradiation, charge separation in TiO_2 results in formation of electrons (e^-) and holes (h^+; $TiO_2 + h\nu \rightarrow n(e^- + h^+)\ TiO_2$) [25]. In Fig. 3A, after irradiation the Blank TiO_2 revealed a strong peak at $g = 2.019$ and a shoulder at 1.991, while the peak at $g = 1.979$ raised and a void at $g = 2.003$ emerged. Holes were trapped at the oxygen atoms of the surface (hydr)oxo groups (e.g. $h^+ + Ti^{4+}\text{-O-}Ti^{4+}\text{-OH} \rightarrow Ti^{4+}\text{-O-}Ti^{4+}\text{-O}^{\bullet} + H^+$) [25]. The peak at $g = 2.019$ is assigned to holes trapped at these surface groups [26–30]. The Ti^{3+} lattice electron-trapping sites originate from both rutile ($g = 1.979$) [26] and anatase ($g = 1.991$) [27].

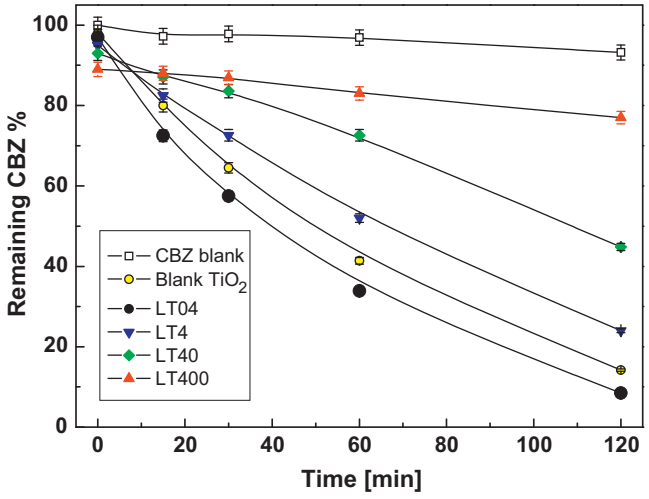

Fig. 1. Carbamazepine (CBZ) photocatalytic degradation with time as measured by HPLC. The CBZ blank is photodegraded in H_2O without any addition of TiO_2 or LHA2.

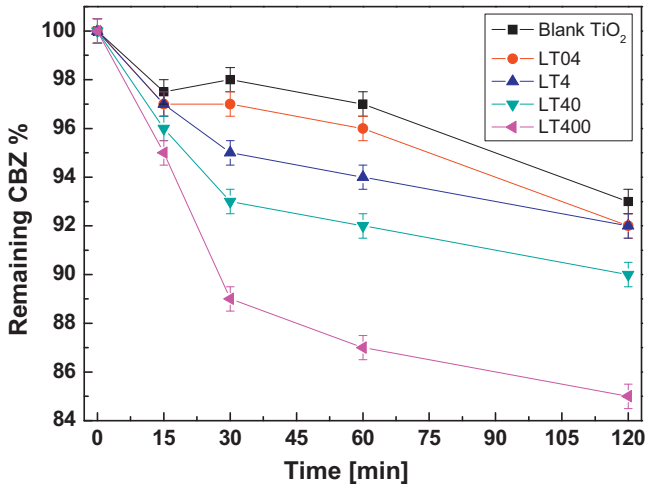

Fig. 2. Carbamazepine (CBZ) adsorption with time as measured by HPLC. All experiments were carried out in the dark to avoid photocatalytic degradation.

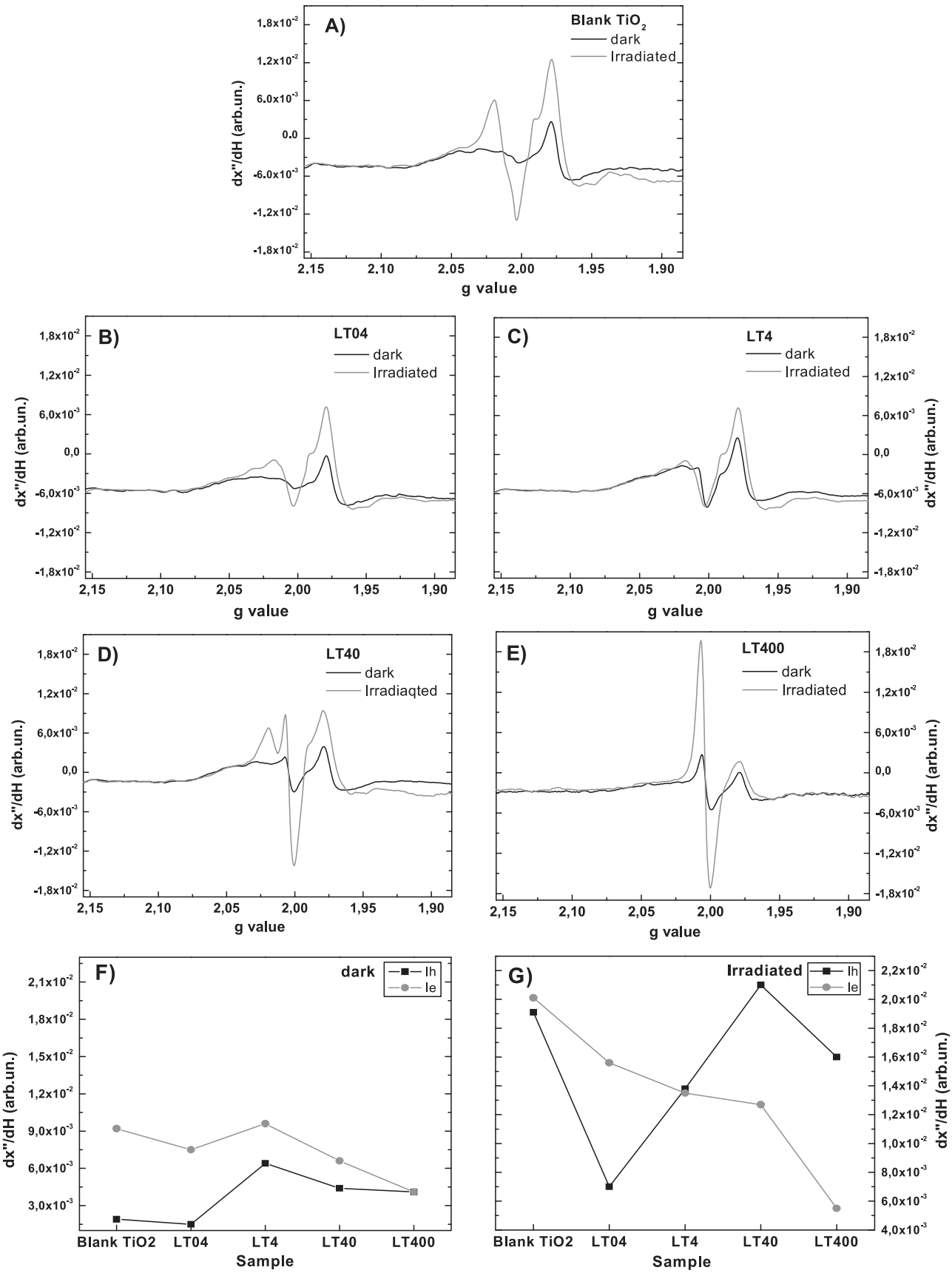

Fig. 3. EPR spectra of Blank TiO_2 and TiO_2 modified with NOM in the dark (black line) and irradiated (grey line). F demonstrates the relative intensity of the holes and electrons in the dark for each sample, while G demonstrates the same when irradiated.

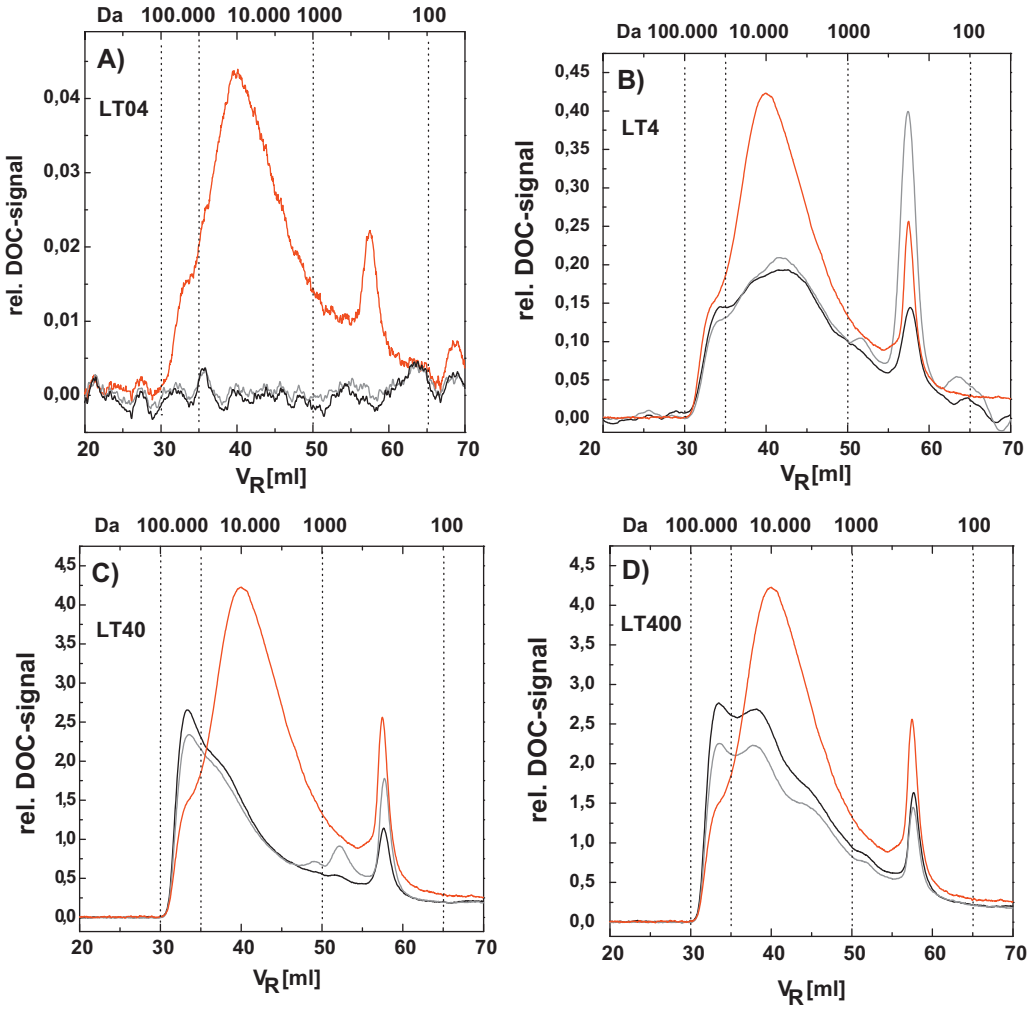

Fig. 4. SEC-OCD chromatograms of LHA2. The red line corresponds to the LHA2 solution. The black line corresponds to the remaining LHA2 solution that was not adsorbed on the TiO_2. The grey line is the matter in solution of the black line matter after 2 h of irradiation. The difference between the red and the black line corresponds to the organic carbon adsorbed on TiO_2 of each sample. The solutions in D were diluted 10 times, not to exceed the detection limit.

In Fig. 3B, after irradiation the LT04 showed a significant difference, as the peak at $g = 2.019$ was greatly reduced. This indicates that this material possessed much more electrons than holes on its surface. LT4 in Fig. 3C revealed almost no difference in between the dark and the irradiated phase. Both spectra were similar to the irradiated spectrum of Fig. 3B. This represents an indication of electron transfer from the LHA2 molecule to the TiO_2 surface. For LT40 (Fig. 3D) once again the irradiated phase was completely different than the dark one. The emerging peak at $g = 2.019$, indicated holes (h^+) trapped on the surface groups, but there was also another peak emerging at $g = 2.007$. This peak probably corresponds to the humic-type oxygen-based radical of LHA2 with g value 2.040 ± 0.005. For LT400 (Fig. 3E), the peak at $g = 2.007$ increased much more than in LT40, revealing the nature of the humic-type oxygen-based radical. However, in LT400, the peak at $g = 1.979$ is greatly reduced, even in the dark, when compared to the Blank TiO_2 (Fig. 3A). This suggests an electron transfer from the TiO_2 surface to the humic molecule. Fig. 3F also reveals that in the dark each material possesses more electrons on the TiO_2 molecule than holes. However, this situation changes significantly after irradiation (Fig. 3G). For both Blank TiO_2 and LT4, there is no difference between the number of electrons and hole sites, when for LT40 and LT400 the electron sites are fewer than hole sites, LT04 acts completely different, bearing much more electron sites than hole sites. These data indicate the different catalytic behavior of these materials towards CBZ degradation, as shown in Fig. 1.

It is well known that the adsorbed molecular oxygen at the catalyst surface is reduced by conduction band electrons (e_{cb}^-) to yield reactive oxygen species (ROS) such as $O_2\bullet^-/HO_2\bullet$ and H_2O_2. The generated hydrogen peroxide interacts with the TiO_2 surface to form $\equiv Ti^{IV}$-OOH surface complexes, which can ultimately produce hydroxyl radicals upon UV or even visible light irradiation [31]. The •OH radical is a powerful oxidizing agent that may react with a wide range of adsorbed organic substances present at or near the TiO_2 surface [32]. The reason for the larger CBZ degradation for LT04 than for Blank TiO_2 (Fig. 1) may then be the excess of electrons produced against holes.

3.4. SEC-OCD chromatography

In order to obtain information about the humic fraction that adsorbs onto the TiO_2 surfaces, size exclusion chromatography (SEC) with organic carbon detection (OCD) was used. The SEC-OCD profiles of LHA2 solutions at different concentrations are marked with red line in Fig. 4. Four different ratios of LHA2:TiO_2 were introduced. After adsorption on the TiO_2 particles, the remaining solution was measured. The grey lines correspond to the solutions of the black lines after 60 min irradiation by the solar UV simulator

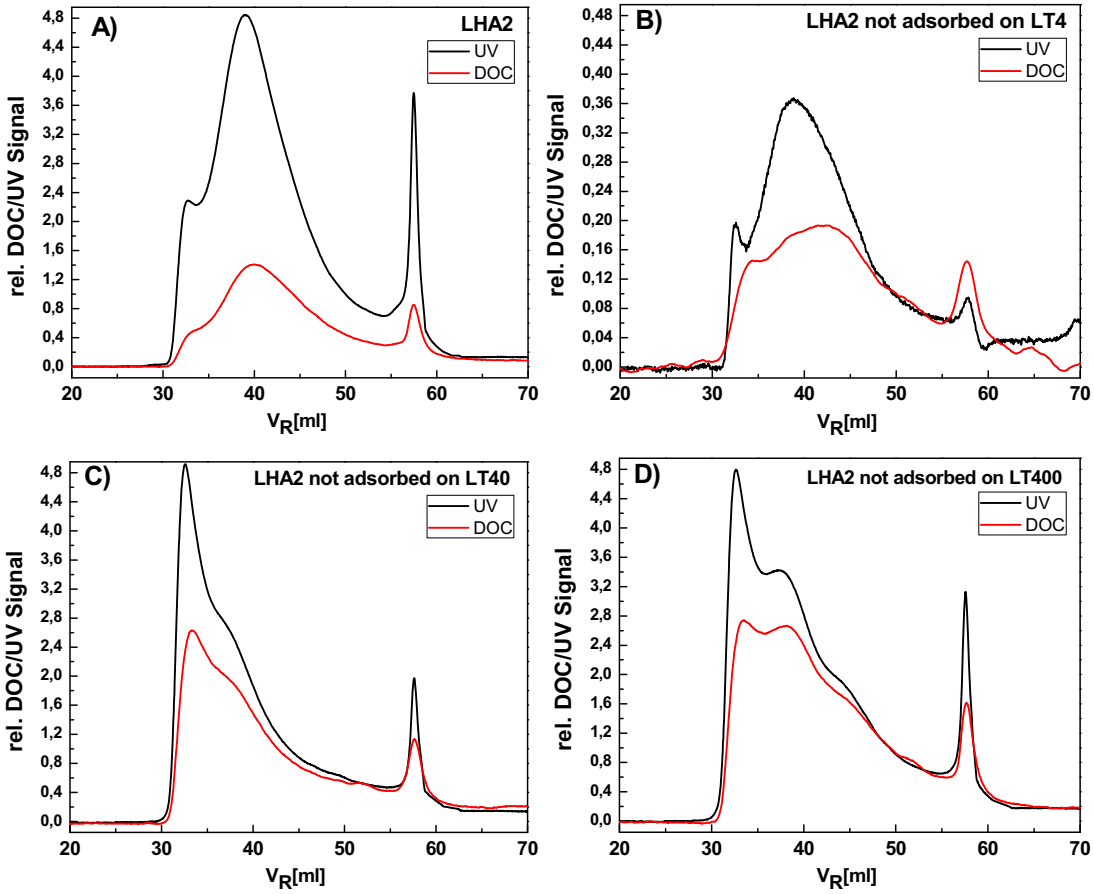

Fig. 5. SEC-OCD chromatograms of LHA2 both by DOC (red line) and UV_{254} (black line) detector to obtain SUVA ratio. (A) LHA2 solution with SUVA 3.7. (B) Remaining LHA2 solution that was not adsorbed on the TiO_2 for the LT4 ratio. SUVA of (B) is 1.3. (C) Remaining LHA2 solution that was not adsorbed on the TiO_2 for the LT40 ratio. SUVA of (C) is 1.2. Finally, (D) remaining LHA2 solution that was not adsorbed on the TiO_2 for the LT400 ratio. SUVA of (D) is 1.3. All solutions were diluted accordingly to obtain chromatograms inside the detection limit with optimum signal to noise ratio.

introduced by Doll et al. [20]. The LHA2 chromatogram showed one peak at 57 mL elution volume that reflects a molecular size between 100 and 1000 Da, one peak at 40 mL (between 1 and 10 kDa) and a shoulder at 33 mL (between 10 and 100 kDa). After adsorption onto TiO_2, the sample with the 400 $\mu g\,g^{-1}$ ratio shows almost no signal, as depicted by the black line in Fig. 4A. This suggests that 85–100% of the NOM was adsorbed on TiO_2. The sample with the 4 $mg\,g^{-1}$ ratio (Fig. 4B) lost most of the dissolved LHA2 matter, but still showed the shoulder at 33 mL, thus indicating that at this ratio, TiO_2 preferably adsorbed small and medium-size NOM fractions reaching an adsorption of 38%. When the ratio raised to 40 $mg\,g^{-1}$ (Fig. 4C), the shoulder at 33 mL became a full. This means that TiO_2 at this ratio not only interacted with NOM by adsorbing small and medium size fractions, but also it activated mechanisms that possibly polymerized the remaining NOM in solution. This phenomenon was repeated also in the 400 $mg\,g^{-1}$ ratio (Fig. 4D). For both ratios, TiO_2 adsorbed first the smaller NOM fractions, as it was observed on hematite by Qin et al. [33]. This agrees with findings by Liu et al., which indicated that due to the complex nature of humic acid (HA), the reactive holes were able to degrade the adsorbed HA into smaller fragments [9]. In Fig. 4C, the adsorption reaches 45% while in Fig. 4D, the adsorption reaches 25%. From Fig. 4, it is clear that after 60 min of irradiation, the loss of the NOM was not greater than 11%. In Fig. 5, the chromatograms of both DOC and UV_{254} detectors are depicted to obtain SUVA ratios, by integration of the chromatogram areas. High SUVA indicates high aromaticity, π–π and/or C=C and C=O bonds. SUVA ratio of LHA2 prior to TiO_2 was 3.7, while in the remaining LHA2 solution that was not adsorbed on TiO_2, all SUVA ratios dropped to 1.2–1.3. This indicates that there are conformational changes on NOM after its interactions with TiO_2, also shown by Tercero et al. [34]. The humic matter not adsorbed on TiO_2 seemed to lose π–π bonds and/or double bonds and became richer in alkyl groups and less hydrophobic.

3.5. NMR spectroscopy

Solid-state ^{13}C CPMAS NMR spectroscopy was used to reveal more about the character of the NOM bound on the TiO_2 surface. NMR spectra of LHA2 and LT400 are shown in Fig. 6. Spectra showed that LHA2 contained 44.9% of alkyl C, 32.9% of aromatic C, of which 8.1% was phenolic C, 8.2% carboxyl and 14% carbonyl C, 3.6% of the latter composed by bridging carbonyl. On the other hand, Fig. 6 indicates that the presence of TiO_2 did not change NOM, but only the percentages of adsorbed carbon groups. Humic matter now bears less carbonyl C (12.1%), with 3% of this being bridging carbonyl C, less carboxyl C (7%) and less aromatic C (27.6%), the latter being 8.1% phenolic C. However, alkyl C was much larger than in the original LHA2 (53.3%). Moreover, LHA2 spectrum revealed that the main peak was at 33 ppm, while this was shifted to 30 ppm in the adsorbed material (LT400). This change reveals methylene units in fast equilibrium between trans and glance conformations, characteristic of molten states [35]. This agrees with the findings by Chen et al. who observed that when humics interact with TiO_2 their conformation changes and TiO_2 mainly adsorbs the phenolic moieties of humic acid [6]. Furthermore, several studies [36–38] have shown that aliphatic chains are the basic structure for humic fractions

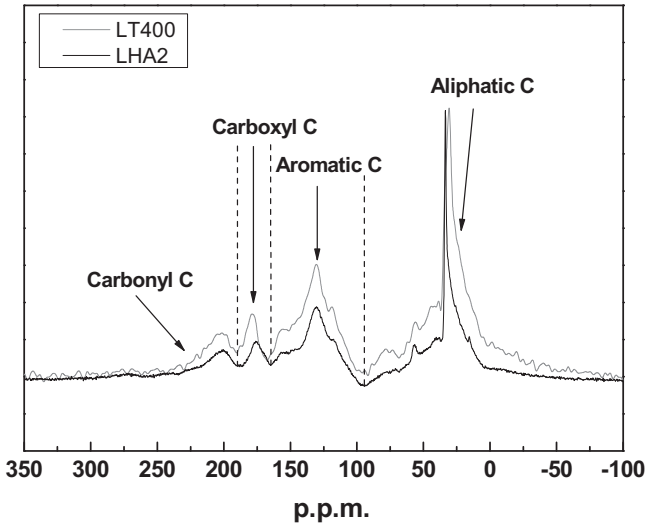

Fig. 6. Solid-state ^{13}C CPMAS-NMR spectra of LHA2 (black line) and LT400 (grey line).

on HA-TiO_2 complexes because aromatic compounds with a large electron density have an increased probability of being attacked by hydroxyl radicals and thus transformed into alkyl chains [39].

3.6. NOM-TiO_2 modification mechanism-in conclusion

Chen et al. attributed the greater Cd(II) adsorption of HA-TiO_2, as compared to that on TiO_2 to the increase of the available adsorption sites generated by the smaller aggregation sizes and better dispersion of TiO_2 nanoparticles in the presence of HA [6]. However, available adsorption sites maybe reduced at greater NOM concentrations due to competition and/or blockage of adsorbing sites by adsorbed HA fractions [40].

Jin-Hui et al. suggested that mechanisms which support TiO_2 effect on the removal of trace organic pollutants in drinking water need further study [41]. Leary et al. proposed a mechanism for the efficiency of TiO_2 modified with activated carbon [18]. Here we generalized this mechanism in order to explain enhancement of organic pollutant degradation by TiO_2 when small amount of NOM is adsorbed. The adsorption of pharmaceuticals onto NOM provides a high concentration of reactants near TiO_2 surfaces, which may then be subjected to photocatalysis possibly by passing through intermediate stages. Without the support of a highly adsorbing matter such as NOM, reactants collide with TiO_2 only by Brownian motion, while NOM ensures the sufficient contact for the photocatalysis to proceed. When the reaction does not occur, the reactants or intermediate products diffuse into solution and can only react when they collide with TiO_2 again.

Our findings demonstrate that when low NOM concentrations are present together with TiO_2 in water, they could enhance the photodegradation rate of organic pollutants like pharmaceuticals, by creating attraction sites on the TiO_2 particles, while high NOM concentrations give the opposite effect, blocking the pharmaceuticals from reaching the TiO_2 particles. It is obvious that a successful application of photocatalysis for wastewater treatment needs solid information on the impact of the water matrix and its components.

Acknowledgments

M.D. was supported by the Bodossaki Foundation. We would like to thank Prof. Yiannis Deligiannakis (University of Ioannina, Greece) for providing access to EPR and support and Matthias Weber (KIT, Germany), for the SEC-OCD analysis and support.

References

[1] U. Diebold, Appl. Phys. A 41 (2002) 1–7.
[2] U. Diebold, Surf. Sci. Rep. 48 (2003) 53–229.
[3] C. Lazau, C. Ratiu, C. Orha, R. Pode, F. Manea, Mater. Res. Bull. 46 (2011) 1916–1921.
[4] P. Guo, X. Wang, H. Guo, Appl. Catal. B: Environ. 90 (2009) 677–687.
[5] K. Yang, B. Xing, Environ. Sci. Technol. 43 (2009) 1845–1851.
[6] Q. Chen, D. Yin, S. Zhu, X. Hu, J. Colloid. Int. Sci. 367 (2012) 241–248.
[7] C. Lazau, C. Ratiu, C. Orha, R. Pode, F. Manea, Mater. Res. Bull. 46 (2011) 1916–1921.
[8] X. Fu, T. Maruyama, T. Sotani, H. Matsuyama, J. Membr. Sci. 320 (2008) 483–491.
[9] S. Liu, M. Lim, R. Fabris, C. Chow, K. Chiang, M. Drikas, R. Amal, Chemosphere 72 (2008) 263–271.
[10] M. Bekbolet, A.S. Suphandag, C.S. Uyguner, J. Photochem. Photobiol. A 148 (2002) 121–128.
[11] J. Fu, M. Ji, Y. Zhao, L. Wang, Sep. Purif. Technol. 50 (2006) 107–113.
[12] H. Tran, J. Scott, K. Chiang, R. Amal, J. Photochem. Photobiol. A 183 (2006) 41–52.
[13] C.S. Uyguner-Demirel, M. Bekbolet, Chemosphere 84 (2011) 1009–1031.
[14] J. Wiszniowski, D. Robert, J. Surmacz-Gorska, K. Miksch, S. Malato, J.-V. Weber, Appl. Catal. B: Environ. 53 (2004) 127–137.
[15] C.S. Uyguner, S.A. Suphandag, A. Kerc, M. Bekbolet, Desalination 210 (2007) 183–193.
[16] J.K. Yang, S.M. Lee, Chemosphere 63 (2006) 1677–1684.
[17] J. Shi, J. Zheng, P. Wu, X. Ji, Catal. Commun. 9 (2008) 1846–1850.
[18] R. Leary, A. Westwood, Carbon 49 (2011) 741–772.
[19] S.U.M. Khan, M. Al-Shahry, W.B. Ingler Jr., Science 297 (2002) 2243–2245.
[20] T.E. Doll, F.H. Frimmel, Chemosphere 52 (2003) 1757–1769.
[21] M. Drosos, M. Jerzykiewicz, Y. Deligiannakis, J. Colloid Int. Sci. 332 (2009) 78–84.
[22] M. Drosos, J.A. Leenheer, A. Avgeropoulos, Y. Deligiannakis, Environ. Sci. Pollut. Res. 21 (2014) 3963–3971.
[23] E. Giannakopoulos, K.C. Christoforidis, A. Tsipis, M. Jerzykiewicz, Y. Deligiannakis, J. Phys. Chem. A 109 (2005) 2223–2232.
[24] M.A. Wilson, in: M.H.B. Hayes, P. MacCarthy, R.L. Malcolm, R.S. Swift (Eds.), Humic Substances II: In Search of Structure, Wiley, New York, 1989, pp. 309–338.
[25] T. Petsi, G.D. Panagiotou, C.S. Garoufalis, C. Kordulis, P. Stathi, Y. Deligiannakis, A. Lycourghiotis, K. Bourikas, Chem. Eur. J. 15 (2009) 13090–13104.
[26] D.C. Hurum, A.G. Agrios, K.A. Gray, T. Rajh, M.C. Thurnauer, J. Phys. Chem. B 107 (2003) 4545–4549.
[27] O.I. Micic, Y. Zhang, K.R. Cromack, A.D. Trifunac, M.C. Thurnauer, J. Phys. Chem. 97 (1993) 13284–13288.
[28] Y. Nakaoka, Y. Nosaka, J. Photochem. Photobiol. A 110 (1997) 299–305.
[29] D.C. Hurum, A.G. Agrios, S.E. Crist, K.A. Gray, T. Rajh, M.C. Thurnauer, J. Electron Spectr. & Rel. Phenom. 150 (2006) 155–163.
[30] O.I. Micic, Y. Zhang, K.R. Cromack, A.D. Trifunac, M.C. Thurnauer, J. Phys. Chem. 97 (1993) 7277–7283.
[31] X. Li, C. Chen, J. Zhao, Langmuir 17 (2001) 4118–4122.
[32] Z. Wang, W. Ma, C. Chen, H. Ji, J. Zhao, Chem. Eng. J. 170 (2011) 353–362.
[33] X. Qin, F. Liu, G. Wang, Chem. Eng. J. 209 (2012) 458–463.
[34] L.A. Tercero-Espinoza, E. ter Haseborg, M. Weber, F.H. Frimmel, App. Catal. B: Environ. 87 (2009) 56–62.
[35] F. López-Carrasquero, A. Martínez de Ilarduya, M. Cárdenas, M. Carrillo, M.-L. Arnal, E. Laredo, C. Torres, B. Méndez, A.J. Müller, Polymer 44 (2003) 4969–4979.
[36] S. Kang, B. Xing, Langmuir 24 (2008) 2525–2531.
[37] K. Wang, B. Xing, J. Environ. Qual. 34 (2005) 342–349.
[38] X. Feng, A.J. Simpson, M.J. Simpson, Environ. Sci. Technol. 40 (2006) 3260–3266.
[39] C. Galindo, P. Jacques, A. Kalt, J. Photochem. Photobiol. A 130 (2000) 35–47.
[40] S. Zhang, T. Shao, S.S.K. Bekaroglu, T. Karanfil, Water Res. 44 (2010) 2067–2074.
[41] Z. Jin-Hui, Proc. Environ. Sci. 12 (2012) 445–452.